

# Substrate Distortion to a Boat Conformation at Subsite -1 Is Critical in the Mechanism of Family 18 Chitinases

Ken A. Brameld and William A. Goddard III\*

Contribution from the Materials and Process Simulation Center, Beckman Institute (139-74), Division of Chemistry and Chemical Engineering, California Institute of Technology, Pasadena, California 91125

Received July 9, 1997. Revised Manuscript Received January 21, 1998

**Abstract:** Using molecular dynamics simulations, we examined the plausible conformations for a hexaNAG substrate bound to the active site of Chitinase A. We find that (i) the hydrolysis mechanism of Chitinase A (a family 18 chitinase from *Serratia marcescens*) involves substrate distortion, (ii) the first step of acid-catalyzed hydrolysis (protonation of the linking anomeric oxygen between GlcNAc residues -1 and +1) requires a boat conformation for the GlcNAc residue at binding subsite -1; (iii) ab initio quantum mechanical calculations (HF/6-31G\*\*) predict that protonation of a GlcNAc in a boat conformation leads to spontaneous anomeric bond cleavage to yield an oxazoline ion intermediate. We also studied several conformations of two possible hydrolysis intermediates: the oxocarbenium ion and the oxazoline ion. Only the oxazoline ion orients in the enzyme active site so as to allow stereoselective attack by water. This leads to retention of configuration in the anomeric product as observed experimentally. It is possible that all family 18 chitinases share a common mechanism. Hence, we suspect that distortion of the substrate into a boat form at subsite -1 is required for any glycosyl hydrolase which has only one acidic residue in the active site. The design of an inhibitor for these systems based on the boat distorted sugar conformation is discussed.

## 1.0 Introduction

Chitin, a  $\beta$  (1,4)-linked *N*-acetylglucosamine (GlcNAc) polysaccharide, is a major structural component of fungal cell walls and the exoskeletons of invertebrates, including insects and crustaceans. This linear polymer may be degraded through the enzymatic hydrolysis action of chitinases. Chitinases have been found in a wide range of organisms including bacteria,<sup>1,2</sup> plants,<sup>3</sup> fungi,<sup>4</sup> insects,<sup>5</sup> and crustaceans.<sup>6</sup> For those organisms that utilize the structural properties of chitin, chitinases are critical for the normal life cycle functions of molting and cell division.<sup>7,8</sup> In addition, plants produce chitinases as a defense against fungal pathogens.<sup>3,9</sup> Because chitin is not found in vertebrates, it has been suggested that inhibition of chitinases may be used for the treatment of fungal infections and human parasitosis.<sup>10</sup>

On the basis of amino acid sequence, the glycosyl hydrolases have been classified into 45 families.<sup>11</sup> Using this classification

method, the chitinases form families 18 and 19 which are unrelated, differing in structure and mechanism. Sequence analysis shows little homology between these classes of chitinases. Family 19 chitinases (found in plants) share the bilobal  $\alpha+\beta$  folding motif of lysozyme, which forms a well-defined substrate binding cleft between the lobes.<sup>12</sup> In contrast, family 18 chitinases share two short sequence motifs which form the catalytic ( $\beta\alpha$ )<sub>8</sub>-barrel active site.<sup>13</sup> Family 18 chitinases with diverse sequences have been isolated from a wide range of eukaryotes and prokaryotes. There are two general mechanistic pathways for acid-catalyzed glycosyl hydrolysis which result in the following: (i) retention of the stereochemistry of the anomeric oxygen at C1' relative to the initial configuration<sup>14</sup> (see Scheme 1) or (ii) inversion of the stereochemistry (see Scheme 2).

An example of the retaining mechanism is hen egg white lysozyme (HEWL), which has been shown to require two acidic residues, one of which is protonated.<sup>15</sup> This mechanism is believed to proceed as follows.<sup>16,17</sup> The  $\beta$ -(1,4)-glycosidic oxygen is first protonated (leading to an *oxocarbenium ion intermediate*) which is stabilized by a second carboxylate (either through covalent or electrostatic interactions). Nucleophilic attack by water yields the hydrolysis product, which necessarily *retains* the initial anomeric configuration. This is commonly

(1) Watanabe, T.; Suzuki, K.; Oyanagi, W.; Ohnishi, K.; Tanaka, H. *J. Biol. Chem.* **1990**, *265*, 15659–15665.

(2) Perrakis, A.; Tews, I.; Dauter, Z.; Oppenheim, A. B.; Chet, I.; Wilson, K. S.; Vorgias, C. E. *Structure* **1994**, *2*, 1169–1180.

(3) Collinge, D. B.; Kragh, K. M.; Mikkelsen, J. D.; Nielsen, K. K.; Rasmussen, U.; Vad, K. *Plant. J.* **1993**, *3*, 31–40.

(4) Bartnicki-Gracia, S. *Annu. Rev. Microbiol.* **1968**, *22*, 87–108.

(5) Kramer, K. J.; Dziadik-Turner C.; Koga, D. In *Comprehensive Insect Physiology, Biochemistry, and Pharmacology: Integument, Respiration, and Circulation*, 1st ed.; Kerkut, G. A., Gilbert, L. I., Eds.; Pergamon Press: Oxford, New York, 1985; Vol. 3.

(6) Koga, D.; Isogai, A.; Sakuda, S.; Matsumoto, S.; Suzuki, A.; Kimura, S.; Ide, A. *Agric. Biol. Chem.* **1987**, *51*, 471–476.

(7) Fukamizo, T.; Kramer, K. J. *Insect Biochem.* **1985**, *15*, 141–145.

(8) Kuranda, M. J.; Robbins, P. W. *J. Biol. Chem.* **1991**, *266*, 19758–16767.

(9) Boller, T.; Gehri, A.; Mauch, F.; Vogeli, U. *Planta* **1983**, *157*, 22–31.

(10) Robertus, J. D.; Hart, P. J.; Monzingo, A. F.; Marcotte, E.; Hollis, T. *Can. J. Bot.* **1995**, *73*, S1142–S1146.

(11) Henrissat, B.; Bairoch, A. *Biochem. J.* **1993**, *293*, 781–788.

(12) (a) Hart, P. J.; Pflugger, H. D.; Monzingo, A. F.; Hollis, T.; Robertus, J. D. *J. Mol. Biol.* **1995**, *248*, 402–413. (b) Monzingo, A. F.; Marcotte, E. M.; Hart, P. J.; Robertus, J. D. *Nat. Struct. Biol.* **1996**, *3*, 133–140.

(13) Terwisscha van Scheltinga, A. C.; Hennig, M.; Dijkstra, B. W. *J. Mol. Biol.* **1996**, *262*, 243–257.

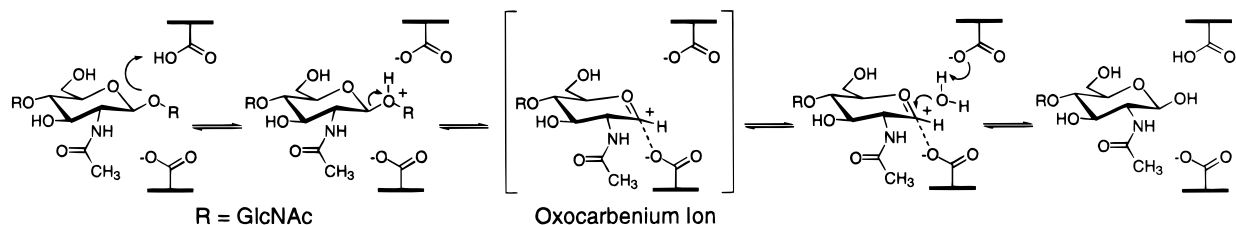
(14) Davies, G.; Henrissat, B. *Structure* **1995**, *3*, 853–859.

(15) Phillips, D. C. *Proc. Natl. Acad. Sci. U.S.A.* **1967**, *57*, 484–495.

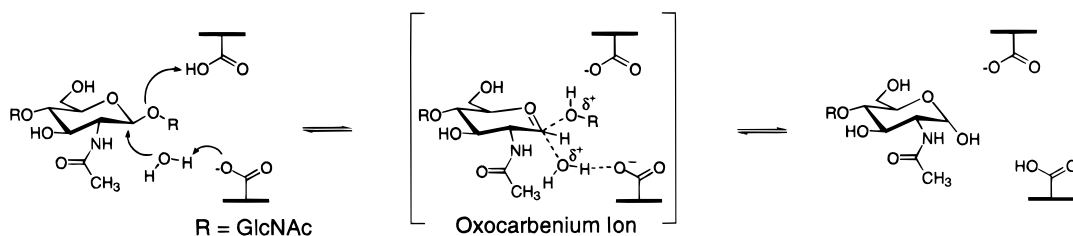
(16) Sinnott, M. L. *Chem. Rev.* **1990**, *90*, 1171–1202.

(17) McCarter, J. D.; Withers, S. G. *Curr. Opin. Struct. Biol.* **1994**, *4*, 885–892.

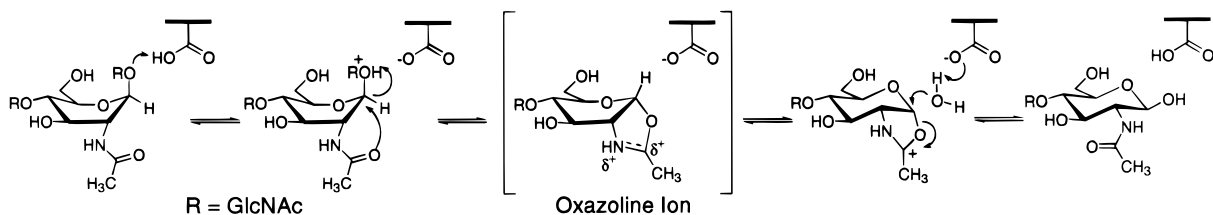
**Scheme 1.** Double-Displacement Hydrolysis Mechanism Which Requires Two Acidic Residues in the Active Site and Leads to Retention of the Anomeric Configuration



**Scheme 2.** Single-Displacement Mechanism Which Requires Only One Acidic Residue in the Active Site and Results in Inversion of the Anomeric Configuration



**Scheme 3.** Anchimeric Stabilization Hydrolysis Mechanism<sup>24</sup> of Family 18 Chitinases Where the Substrate Is Distorted to a Boat Conformation and the Oxazoline Ion Intermediate Is Stabilized through Anchimeric Assistance from the Neighboring C2' *N*-Acetyl Group



referred to as the *double displacement* mechanism of hydrolysis (see Scheme 1).<sup>14–18</sup>

Although the X-ray crystal structure of a family 19 chitinase reveals a lysozyme-like fold (suggesting a double displacement mechanism<sup>12</sup>), the hydrolysis products for two family 19 chitinases show *inversion* of the anomeric configuration.<sup>19,20</sup> This leads to the second commonly discussed hydrolysis mechanism: a *concerted single displacement reaction* in which a bound water molecule acts as the nucleophile (see Scheme 2). The crystal structure suggests that the second catalytic carboxylate may be sufficiently close to allow coordination of a water molecule consistent with a single displacement mechanism.

Family 18 chitinases have been reported to yield hydrolysis products which *retain* the anomeric configuration at C1'.<sup>21</sup> However, the X-ray crystal structure of two family 18 chitinases reveals no second acidic residue in the active site capable of stabilizing the oxocarbenium ion.<sup>2,22</sup> Thus, neither the single nor double displacement mechanism is consistent with the observed structure and hydrolysis products. An increasing body of experimental<sup>23</sup> and theoretical evidence<sup>24</sup> points to an oxazoline ion intermediate formed through anchimeric assistance

by the neighboring *N*-acetyl group (see Scheme 3) as being the likely mechanism for family 18 chitinases. Such an intermediate alleviates the need for a second acidic residue. In solution, spontaneous acid-catalyzed hydrolysis of 2-acetamido-substituted polysaccharides have been reported to occur through anchimeric assistance.<sup>25</sup>

The oxazoline double displacement mechanism may not be unique to family 18 chitinases. The X-ray structure of a bacterial chitinase<sup>26</sup> (family 20) complexed with the unhydrolyzed natural substrate revealed that the glycosidic bond to be cleaved was in a “quasi-axial” orientation. In addition, the C2' *N*-acetyl group was found to be in a position to allow the formation of an oxazoline ion intermediate. A similar substrate distortion was observed for endoglucanase I,<sup>27</sup> a cellulase from family 7, complexed with a nonhydrolyzable thiooligosaccharide substrate analogue. As in the chitinase structure, the substrate occupied subsites spanning the points of enzymatic cleavage and revealed a distortion in the sugar conformation at the cleavage site. Once again, a “quasi-axial” orientation for the glycosidic bond was observed and the nucleophile of endoglucanase I was in a similar position to the C2' *N*-acetyl group of the chitinase structure.

We report here molecular dynamics (MD) simulations of a family 18 bacterial chitinase (Chitinase A from *Serratia*

(18) Koshland, D. E. *Biol. Rev.* **1953**, *28*, 416.

(19) Fukamizo, T.; Koga, D.; Goto, S. *Biosci. Biotech. Biochem.* **1995**, *59*, 311–313.

(20) Iseli, B.; Armand, S.; Boller, T.; Neuhaus, J.-M.; Henrissat, B. *FEBS Lett.* **1996**, *382*, 186–188.

(21) Armand, S.; Tomita, H.; Heyraud, A.; Gey, C.; Watanabe, T.; Henrissat, B. *FEBS Lett.* **1994**, *343*, 177–180.

(22) Terwisscha van Scheltinga, A. C.; Kalk, K. H.; Beintema, J. J.; Dijkstra, B. W. *Structure* **1994**, *2*, 1181–1189.

(23) Terwisscha van Scheltinga, A. C.; Armand, S.; Kalk, K. H.; Isogai, A.; Henrissat, B.; Dijkstra, B. W. *Biochemistry* **1995**, *34*, 15619–15623.

(24) Brameld, K. A.; Shrader, W. D.; Imperiali, B.; Goddard, W. A., III Submitted for publication.

(25) (a) Piskiewicz, D.; Bruice, T. C. *J. Am. Chem. Soc.* **1967**, *89*, 6237–6243. (b) Piskiewicz, D.; Bruice, T. C. *J. Am. Chem. Soc.* **1968**, *90*, 2156–2163.

(26) Tews, I.; Perrakis, A.; Oppenheim, A.; Dauter, Z.; Wilson, K. S.; Vorgais, C. E. *Nat. Struct. Biol.* **1996**, *3*, 638–648.

(27) Sulzenbacher, G.; Driguez, H.; Henrissat, B.; Schulein, M.; Davies, G. J. *Biochemistry* **1996**, *35*, 15280–15287.

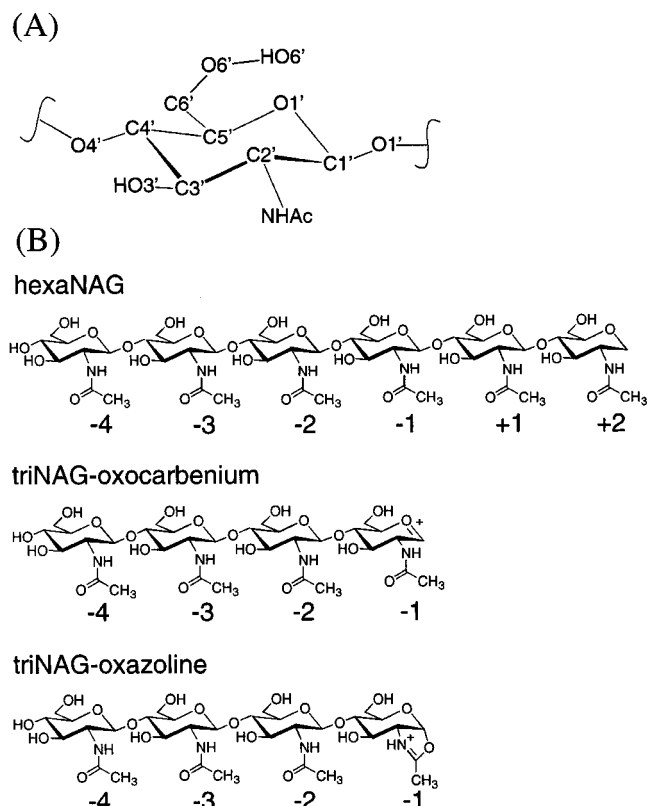


**Figure 1.** Structures and sugar-labeling scheme used for the hexaNAG substrate and the triNAG-oxocarbenium ion and triNAG-oxazoline ion intermediates. Sugars are numbered  $-4$  through  $+2$  from the nonreducing end as is the current convention.

*marcescens*). We have investigated initial substrate binding and the possible resulting hydrolysis intermediates. We find the hexaNAG substrate is forced to distort to a boat sugar geometry at subsite  $-1$ , prior to protonation, which then leads to spontaneous anomeric bond cleavage and subsequent formation of an oxazoline ion.

Section 2 describes the computational details, and section 3 reports the simulation results. Section 4 discusses the implications of the simulation results upon understanding of the hydrolysis mechanism and examines issues important for the design of a new class of inhibitor.

## 2.0 Methods

**2.1 Simulation Methods.** All MD simulations were carried out using the MSC-PolyGraf<sup>28</sup> program with the Dreiding force field (FF).<sup>29</sup> Averaged charge equilibrium (QE) charges<sup>30</sup> were used for all GlcNAc residues. Charges for the oxocarbenium and oxazoline ions are from ab initio quantum mechanics (QM) calculations (HF/6-31G\*\*).<sup>24</sup> Figure 2 illustrates the FF atom types and charges used in the simulation. Charges for the amino acid side chains are from CHARMM.<sup>31</sup> For protonated Glu 315, the net charge was neutralized, with the following assignment: CA 0.05, N  $-0.40$ , H 0.25, C 0.60, O  $-0.55$ , CB  $-0.10$ , HB 0.05, CG  $-0.25$ , HG 0.05, CD 0.40, OE1  $-0.30$ , OE2  $-0.30$ , HOE 0.35.

A standard Coulomb potential was used without a distance dependent dielectric constant, and all nonbond interactions were considered explicitly. A nonbond cutoff of 9.5 Å was used during MD simulations

(28) MSC-Biograp/Polygraf is the MSC version 3.3 of the software originally distributed by Molecular Simulations Inc., San Diego, CA.

(29) Mayo, S. L.; Olafson, B. D.; Goddard, W. A., III *J. Phys. Chem.* **1990**, *94*, 8897–8909.

(30) Rappe, A. K.; Goddard, W. A., III *J. Phys. Chem.* **1991**, *95*, 3358–3363.

(31) Bruccoleri, R. E.; Olafson, B. D.; States, D. J.; Swaminathan, S.; Karplus, M. *J. Comput. Chem.* **1983**, *4*, 187–217.

and extended to 13.5 Å for single-point energy calculations. Solvation energies were estimated using the continuum solvent model in the Delphi program.<sup>32</sup>

The ab initio QM calculations (HF/6-31G\*\*\*) were carried out with the PS-GVB program<sup>33–35</sup> from Schrödinger, Inc. During geometry optimization of the two protonated methyl-GlcNAc conformations, the O4'–C1'–O1'–C(methyl) torsion was constrained to be 120°. This constraint was necessary to prevent free rotation about the anomeric bond and proton transfer from O1' to the *N*-acetyl group carbonyl oxygen. An analogous conformational constraint occurs for the hexaNAG substrate upon binding to Chitinase A.

**2.2 Starting Structures.** Crystal structures have been solved for hevine and Chitinase A,<sup>2</sup> both family 18 chitinases. There is little structural information known regarding substrate binding to Chitinase A. However, several structures for hevine have been reported which include complexes with triNAG<sup>22</sup> and allosamidin.<sup>23</sup> We used the detailed knowledge of the hevine system to aid in the initial docking of the ligands to Chitinase A. A sequence alignment of several members of the family 18 glycosyl hydrolases<sup>13</sup> simplified the task of structural alignment between Chitinase A and hevine. The following residues were included in a least-squares coordinate match: Tyr 6, Asp 123, Asp 125, Glu 127, Tyr 183, and Trp 255 of the hevine active site and Tyr 163, Asp 311, Asp 313, Glu 315, Tyr 390, and Trp 539 of Chitinase A.

The triNAG/hevine complex structure served as a starting point for the structure of hexaNAG residues  $-4$ ,  $-3$ , and  $-2$ .<sup>36</sup> The remaining three GlcNAc residues ( $-1$ ,  $+1$ , and  $+2$ ) were built individually and optimized through simulated annealing. The allosamidin/hevine complex was used as a template for the *N*-acetyl geometry at subsite  $-1$ . In total, six different starting conformations for GlcNAc residues  $-1$  through  $+2$  were examined. Each conformation was subjected to 10 annealing cycles during which the temperature was raised from 0 to 350 K and back to 0 K in increments of 50 K every 100 fs for a total of 2.1 ps. This resulted in only two distinct conformations, which differed only at subsite  $-1$ , denoted as  $-1$ -chair and  $-1$ -boat.

The structures of the intermediates were based on the equilibrated hexaNAG models. GlcNAc residues  $+1$  and  $+2$  were removed, and the correct changes in atom hybridization were applied to generate an oxocarbenium ion or oxazoline ion.

Counterions and crystallographic water molecules were included during all simulations to ensure a net neutral charge. Water molecules in van der Waals (vdW) contact with the docked ligand were moved to avoid high-energy starting conformations. Residues 24–150 were deleted from the simulation. These residues form the N-terminal domain which has unknown function. On the basis of a 6 Å distance cutoff from the bound hexaNAG substrate, the following residues were movable during all simulations: 163–172, 189–191, 204–213, 228–231, 273–277, 311–316, 361–364, 386–391, 442–446, 470–478, and 539–543. All other residues were fixed.

## 3.0 Results

**3.1 Simulations of hexaNAG Substrate Binding.** The binding of a hexaNAG substrate (Figure 1) to Chitinase A was

(32) Honig, B.; Nicholls, A. *Science* **1995**, *268*, 1144–1149. Software code is available from the Department of Biochemistry, Columbia University.

(33) Greeley, B. H.; Russo, T. V.; Mainz, D. T.; Friesner, R. A.; Langlois, J.-M.; Goddard, W. A., III; Donnelly, R. E.; Ringnalda, M. N. *J. Chem. Phys.* **1994**, *101*, 4028–4041.

(34) Ringnalda, M. N.; Langlois, J.; Greeley, B. H.; Murphy, R. B.; Russo, T. V.; Cortis, C.; Muller, R. P.; Marten, B.; Donnelly, R. E.; Mainz, D. T.; Wright, J. R.; Pollard, W. T.; Cao, Y.; Won, Y.; Miller, G. H.; Goddard, W. A., III; Friesner, R. A. PS-GVB 2.24 from Schrödinger Inc., 1996.

(35) Muller, R. P.; Langlois, J.-M.; Ringnalda, M. N.; Friesner, R. A.; Goddard, W. A., III *J. Chem. Phys.* **1994**, *100*, 1226–1235. Murphy, R. B.; Friesner, R. A.; Ringnalda, M. N.; Goddard, W. A., III *J. Chem. Phys.* **1994**, *101*, 2986–2994. Langlois, J.-M.; Yamasaki, T.; Muller, R. P.; Goddard, W. A., III *J. Phys. Chem.* **1994**, *98*, 13498–13505.

(36) The sugar residues are labeled  $-4$  to  $+2$  from the nonreducing end as is the current convention. Davies, G. J.; Wilson, K. S.; Henrissat, B. *Biochem. J. Lett.* **1997**, *321*, 557–559.

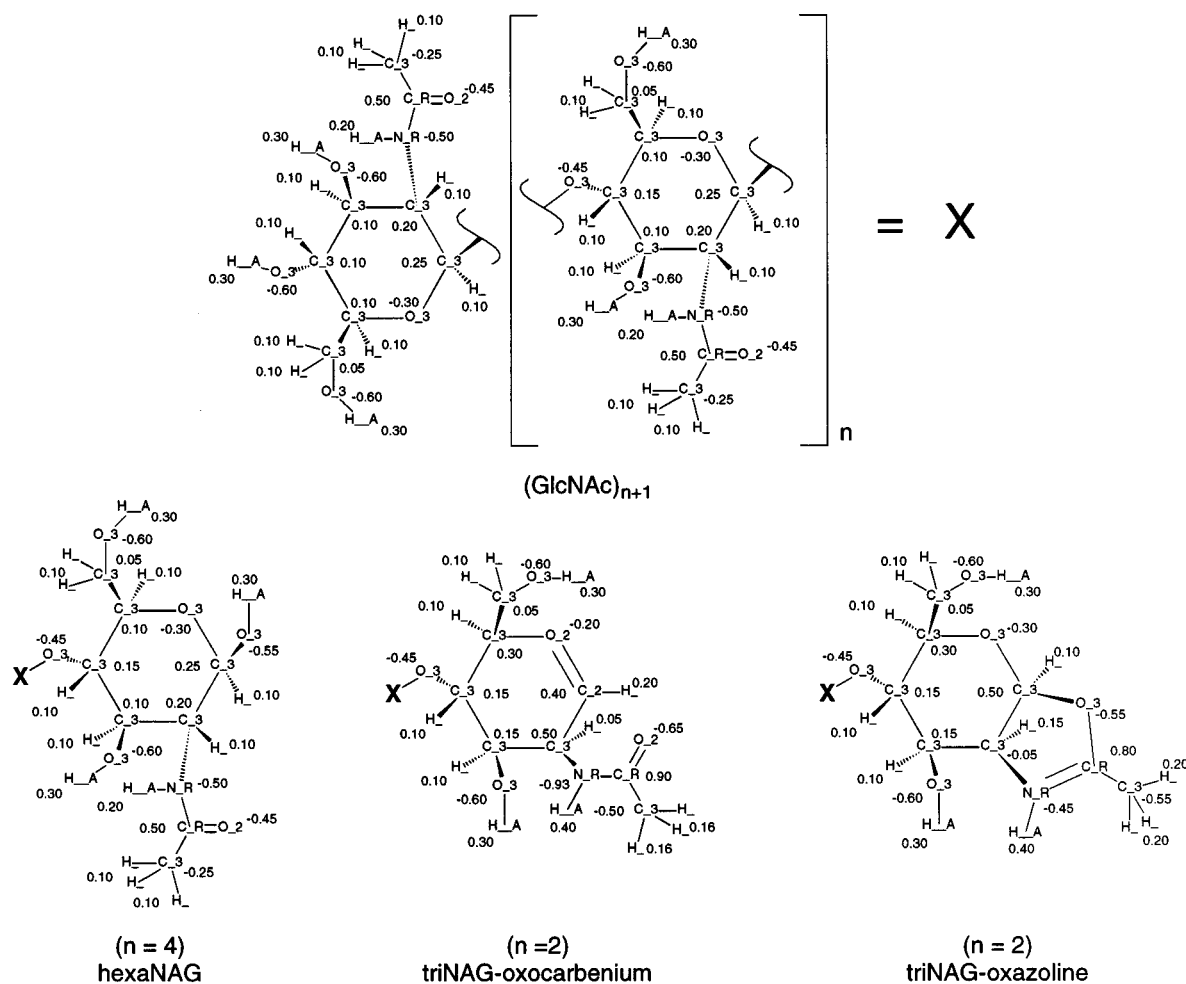


**Figure 2.** Atomic charges and force field atom types used for the simulation. X denotes a GlcNAc residue in the middle of the chain. The chain may be terminated in one of three ways: hexaNAG, a GlcNAc residue; triNAG-oxocarbenium, an oxocarbenium ion; triNAG-oxazoline, an oxazoline ion.

studied using MD simulations. Starting from the reported X-ray crystal structures of both the triNAG/hevamine<sup>22</sup> and the alloamidin/hevamine complex,<sup>23</sup> a tetraNAG substrate was docked to Chitinase A and two additional NAG residues were built and optimized. Six different binding conformations for hexaNAG were constructed, each differing in the geometry of the sugars bound at subsites -1 through +2 as these sites could not be extrapolated from the hevamine crystal structures. Simulated annealing cycles, carried out for each conformation and the surrounding binding site side chains, resulted in only two globally different binding modes. These differed primarily at the sugars bound in subsites -2 and -1 and have been labeled -1-boat and -1-chair in reference to the pyranose ring conformation of sugar residue -1.

One hundred picoseconds of MD was carried out on both optimized hexaNAG conformations. The binding site residues (Figure 3), crystallographic waters, counterions, and hexaNAG substrate were all free to move during the simulation. Both the -1-chair and -1-boat conformations were stable, and little deviation from the crystal structure was observed for the binding site residues (Table 1). For the -1-boat conformation, analysis of an ensemble of snapshots taken at regular time intervals reveals considerable mobility at the hexaNAG termini (sugars -4 and +2) while the central residues are tightly bound (Table 2). The -1-chair conformation shows greater flexibility or instability compared to the -1-boat conformation, greatest at sugar -4 and decreasing to sugar +2.

The -1-boat binding geometry is stabilized through a series of specific hydrogen bonds between each GlcNAc residue and the binding site of the enzyme (Figure 3). The O6' of sugar -4 interacts with a counterion bound to Asp 230. The *N*-acetyl carbonyl of sugar -3 forms a hydrogen bond to the side chain of Thr 276 while the O6' hydrogen bonds to Asn 474. Hydrophobic contacts are also made with Trp 167. The *N*-acetyl amide of sugar -2 donates a hydrogen bond to Glu 473 while the carbonyl accepts a hydrogen bond from Arg 172. Nonspecific contacts are made with the hydrophobic "floor" of the binding cleft. Sugar -1 is tightly bound through a hydrogen bond from Tyr 390 to the *N*-acetyl carbonyl and from the *N*-acetyl amide to Glu 315 (one oxygen is protonated). There are also critical hydrophobic interactions with Tyr 163 and Trp 539 which *force the -1 sugar into a boat conformation*. Sugar +1 is less tightly bound and forms a hydrogen bond between Arg 446 and the *N*-acetyl carbonyl. Similarly, sugar +2 also makes few specific contacts except for a hydrogen bond between the *N*-acetyl carbonyl and main chain amide hydrogen of Asp 391.

The -1-chair conformation makes fewer stabilizing contacts with the Chitinase A binding site, particularly in the region of sugars -2 and -1 adjacent to the cleavage site. The first two sugars, -4 and -3, are in a similar position to the -1-boat geometry and form the same hydrogen bonds. Sugar -2 is no longer oriented perpendicular to the binding cleft, as observed for the hevamine triNAG complex, but rather has rotated to

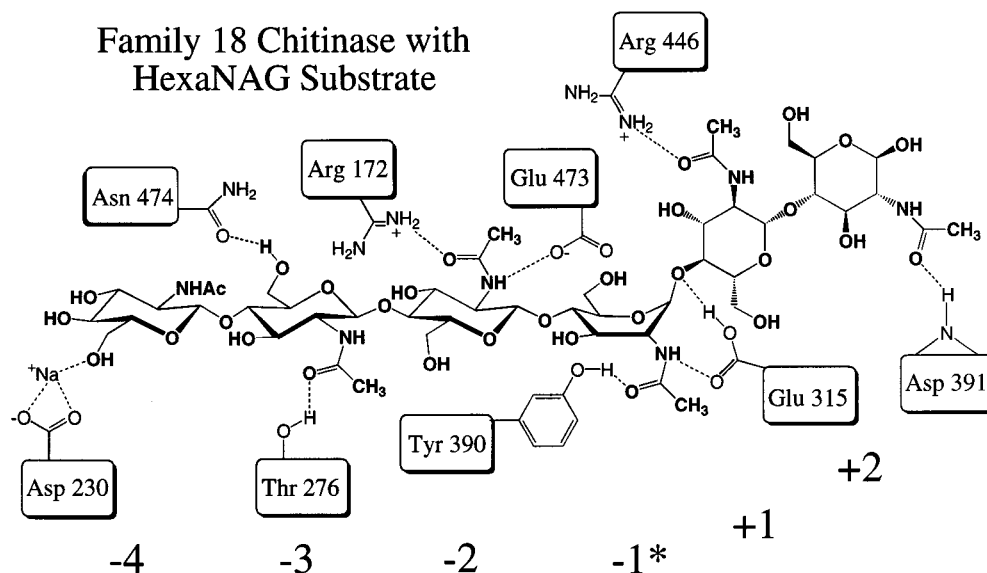


**Figure 3.** A schematic of the hydrogen bonds observed for the  $-1$ -boat hexaNAG binding mode. Note: In this schematic representation Tyr 390 appears to the left of the *N*-acetyl carbonyl oxygen of residue  $-1$ . However, the true structure has this carbonyl group rotated below the plane of the sugar (see Figure 4) with Tyr 390 positioned on the opposite side of the binding cleft. Thus, the hydrogen bond to Tyr 390 helps to position the *N*-acetyl group prior to formation of an oxazoline ion and will not slow catalysis.

**Table 1.** RMS Coordinate Difference ( $\text{\AA}$ ) for Binding Site Residues

substrate	av RMS <sup>a</sup>
hexaNAG ( $-1$ -chair)	1.59
hexaNAG ( $-1$ -boat)	1.43
triNAG-oxocarbenium ( $-1$ -chair)	1.54
triNAG-oxocarbenium ( $-1$ -boat)	1.50
triNAG-oxazoline	1.49
none	2.13

<sup>a</sup> Coordinate RMS difference was calculated as the difference between the crystal structure coordinates<sup>2</sup> and the average position for all non-hydrogen atoms during the MD interval from 30 to 100 ps.

**Table 2.** RMS Coordinate Fluctuation ( $\text{\AA}$ ) from Dynamical Average for HexaNAG Substrate Binding<sup>a</sup>

conformation	binding subsite					
	-4	-3	-2	-1	+1	+2
$-1$ -chair	1.188	0.565	0.568	0.653	0.500	0.346
$-1$ -boat	0.805	0.443	0.340	0.335	0.339	0.512

<sup>a</sup> RMS coordinate fluctuations were calculated as follows: The average structure for the MD interval from 30 to 100 ps was determined. The RMS coordinate differences between this average structure and snapshots taken every 5 ps from 30 to 100 ps were determined. The average of this RMS is reported, separated by sugar residue.

become parallel to the cleft, as is seen for HEWL. This places the *N*-acetyl group toward the binding cleft interior and allows for the formation of only one hydrogen bond from the *N*-acetyl amide to the Trp 275 backbone carbonyl. Facing toward the solvent, HO6' forms a hydrogen bond with Glu 206. Similarly, sugar  $-1$  only makes two hydrogen bonds, one between O3' and Arg 446 and the other between O6' and the *proton* of Glu 315. This greatly limits the possibility of proton transfer to the  $\beta$ -(1,4)-glycosidic oxygen which is the first step in the hydrolysis mechanism. The implications of this result are discussed in greater detail in section 4.1. The final two sugars, +1 and +2, share features with the  $-1$ -boat conformation and form the same transient hydrogen bonds described above.

Relative binding energies for the two hexaNAG conformations are difficult to assess. Many factors influence ligand binding, including solvation energies, entropic consequences of water displacement, and electrostatic interactions. These dif-

**Table 3.** RMS Coordinate Fluctuation ( $\text{\AA}$ ) from Dynamical Average for TriNAG Intermediates<sup>a</sup>

conformation	binding subsite			
	-4	-3	-2	-1
triNAG-oxocarbenium- $-1$ -chair	0.528	0.478	0.704	0.524
triNAG-oxocarbenium- $-1$ -boat	0.414	0.339	0.573	0.257
triNAG-oxazoline	0.445	0.407	1.021	0.267

<sup>a</sup> RMS coordinate fluctuations were calculated as follows: The average structure for the MD interval from 30 to 100 ps was determined. The RMS coordinate differences between this average structure and snapshots taken every 5 ps from 30 to 100 ps were determined. The average of this RMS is reported, separated by sugar residue.

**Table 4.** HexaNAG Binding Energies (kcal/mol)

	$-1$ -boat	$-1$ -chair	$E_{\text{boat}} - E_{\text{chair}}$
MM energy	-39.7	-15.3	-24.4
solvation energy <sup>a</sup>	139.1	108.4	30.7
total energy <sup>b</sup>	99.4	93.1	6.3

<sup>a</sup> Calculated using a continuum solvation method with the Delphi<sup>29</sup> program. <sup>b</sup> Total energy is the sum of the MM and solvation energies.

ficulties are made even more complex as a result of the large number of possible hydrogen-bond conformations available to carbohydrates which result in many local minima of similar energy. However, we have attempted to determine the energetic differences between the two binding modes (see Table 4). We calculate that the  $-1$ -boat conformation has an internal energy 24.4 kcal/mol *lower* than the  $-1$ -chair conformation. To estimate the differential solvation energy, we used a continuum solvation approximation<sup>32</sup> for each conformation in water (both bound to the enzyme and free in solution). We calculate that the  $-1$ -chair conformation has a solvation energy 30.7 kcal/mol more *favorable* than the  $-1$ -boat conformation. Combining these two contributions, we estimate that the  $-1$ -chair geometry is preferred by 6.3 kcal/mol. Probably the uncertainty in these estimated energies is comparable to this difference, indicating that both conformations are thermodynamically accessible.

**3.2 Simulations of Bound Intermediates.** Following binding of the chitin substrate, any acid-catalyzed hydrolysis

mechanism requires a proton transfer from Glu 315 to the  $\beta$ -(1,4)-glycosidic oxygen linking sugars  $-1$  and  $+1$ . Upon proton transfer and the departure of chitobiose (formed from the  $+1$  and  $+2$  sugars), there remains a positively charged intermediate. Starting from the two hexaNAG conformations discussed above, three intermediates are possible: two oxocarbenium ion intermediates, which differ in the geometry of the *N*-acetyl group, and an oxazoline ion. We previously studied the aglycones of these intermediates using ab initio QM methods.<sup>24</sup> We found that the oxazoline ion intermediate was substantially ( $\sim 18$  kcal/mol) lower in energy both when isolated and while bound to the active site of hevamine, also a family 18 chitinase. We have now extended this work to include the full enzyme and the triNAG-substituted intermediates in MD simulations of Chitinase A.

**3.2.1 Binding of the  $-1$ -Chair-Derived Oxocarbenium Ion.** Starting from the  $-1$ -chair hexaNAG structure, sugars  $+1$  and  $+2$  were removed and sugar  $-1$  was converted to an oxocarbenium ion. Following a series of annealing cycles, 100 ps of MD was carried out.

The positively charged  $C1' - O5'$  is stabilized by interactions with Glu 315 and Asp 391. However, to attain these favorable interactions, the specific hydrogen bonds observed for sugars  $-4$  through  $-2$  are disrupted. Indeed, only a few hydrogen bonds remain intact and considerable mobility of sugars  $-4$  through  $-2$  is observed during the simulation (Table 3).  $HO6'$  and  $HO4'$  of sugar  $-4$  form transient hydrogen bonds to Glu 208. Arg 172 now forms a hydrogen bond with  $O6'$  of sugar  $-3$  instead of the *N*-acetyl carbonyl group of sugar  $-2$ . Arg 446 replaces Arg 172 and forms a hydrogen bond to the *N*-acetyl carbonyl group of sugar C.

No water molecules were observed near the oxocarbenium ion during the simulation. However, it is readily observable that the positioning of the oxocarbenium ion in the active site cleft, relative to Glu 315 and Asp 391, will result in little stereoselectivity during nucleophilic attack by water.

**3.2.2 Binding of the  $-1$ -Boat-Derived Oxocarbenium and Oxazoline Ion.** The simulation results for the  $-1$ -boat-derived oxocarbenium ion and oxazoline ion intermediates were very similar. The docked structures were generated from the hexaNAG  $-1$ -boat model, following removal of sugars  $+1$  and  $+2$ . A series of annealing cycles were followed by 100 ps of MD.

The interactions of sugars  $-4$  through  $-2$  with specific residues of the binding site of Chitinase A for both intermediates were analogous to the hexaNAG simulation. Only the hydrogen bond from Asn 474 to  $O6'$  of sugar  $-3$  was missing. This was replaced by Arg 172, leaving the total number of hydrogen bonds unchanged. This is reflected in the greater stability of each of these intermediates over the  $-1$ -chair oxocarbenium ion (Table 3). Occupation of the active site by the oxazoline ion or  $-1$ -boat oxocarbenium ion is stabilized through favorable electrostatic interactions with Glu 315. In addition, hydrogen bonds were observed between  $O6'$  and Arg 446 and from the *N*-acetyl amide to Glu 315.

It is evident from the low root-mean-square (RMS) coordinate fluctuation that the oxazoline ion binds tightly at subsite  $-1$ . This serves to stabilize the oxazoline intermediate and greatly limits the solvent accessible sites. Due to these geometric constraints, nucleophilic attack by water only can lead to retention of the  $\beta$ -anomer, as is observed experimentally.

**3.3 Simulation of Isolated Chitinase A.** As a control study, the same methods were applied to Chitinase A with no substrate or intermediates bound in the active site. The purposes of this

simulation were to ensure that the methods used would generate a stable trajectory and to identify any structural changes that may take place upon substrate binding. We found that the enzyme binding site did remain stable and the overall fold was unchanged. The RMS coordinate difference between the average dynamics structure and the crystal structure was 2.13 Å. This is on average 0.5 Å larger than the value observed for simulations which included a ligand (Table 1).

While no gross structural changes in the binding site were observed, some conformational changes took place during the early preequilibration portion (time = 0–20 ps) of the trajectory. These changes persisted for the remainder of the simulation. The side chains of residues Trp 275 and Trp 167, which form part of the hydrophobic “floor” of the binding site cleft, were very flexible. The largest deviation from the crystal structure was observed for the residues 163–172 and 470–478 which define the walls of the binding site cleft of subsites  $-4$  and  $-3$ . These include several charged side chains (Arg 172, Glu 473, Asp 478) which exhibited a tendency to move toward the solvent and widen the cleft. Little motion was observed in the enzyme active site pocket comprised of residues Asp 313, Glu 315, Met 388, Tyr 390, and Trp 539.

**3.4 Ab Initio QM Calculations for Protonated GlcNAc.** We used ab initio QM (HF/6-31G\*\*) to assess the affects of the  $-1$ -boat substrate distortion upon the energetics of hydrolysis. We optimized the geometry of a protonated GlcNAc sugar residue starting from both a chair and boat conformation. When no geometric constraints were used, free rotation about the glycosidic bond allowed the proton to rotate toward the *N*-acetyl carbonyl, eventually transferring completely. As this rotation is not possible in the chitin polymer, a methyl substitution was made at  $O1'$  (in place of a full neighboring GlcNAc residue) and the C(methyl)- $O1' - C1' - C2'$  torsion was constrained to remain at  $120^\circ$ . This constraint was used for both the chair and boat geometry optimizations.

Starting from a boat conformation of the protonated  $O1' - GlcNAc$  **2** (Figure 6a), a geometry optimization leads to spontaneous glycosidic bond cleavage with subsequent formation of an oxazoline ion-methanol complex, **3** (Figure 6a). In contrast, starting from a chair conformation leads to a stable oxonium ion, **1** (Figure 6a). These interesting results suggest an important role for the  $-1$ -boat substrate distortion observed during the MD simulations. The optimum structure for the protonated chair lies 20.8 kcal/mol higher in energy than the oxazoline complex. While an exhaustive transition state search has not been carried out, a scan of different  $O1' - C1'$  distances did not reveal an energy barrier which would hinder the formation of the oxazoline ion intermediate. The mechanistic implications of these calculations are discussed in section 4.2.

## 4.0 Discussion

We have carried out MD simulations on Chitinase A complexed with various substrate conformations and potential hydrolysis intermediates. Combining these simulations with reported experimental observations, we have been able to make some predictions regarding the hydrolysis mechanism. We find considerable evidence in support of a mechanism in which the substrate is distorted to achieve the boat conformation at subsite  $-1$ , prior to glycosidic bond cleavage. This leads to a double displacement hydrolysis mechanism involving an oxazoline ion intermediate.

**4.1 Proton Donation by Glu 315.** It is generally accepted that the first step of the acid-catalyzed hydrolysis mechanism of Chitinase A involves a proton transfer from Glu 315.<sup>2</sup>

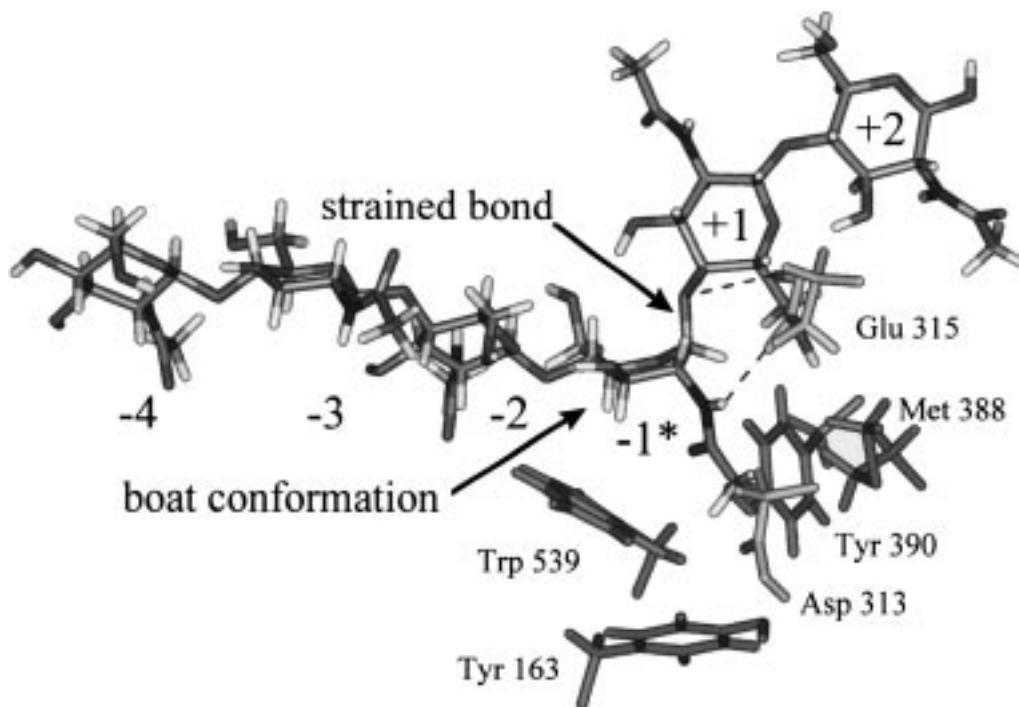


**Figure 4.** The minimum energy structure for the  $-1$ -boat hexaNAG conformation. A boat geometry for GlcNAc residue  $-1$  and the twist between residues  $-1$  and  $+1$  strain the linking glycosidic bond. Glu 315 is found to be oriented so as to allow rapid proton transfer to the linking anomeric oxygen and to form a hydrogen bond with the *N*-acetyl amide.

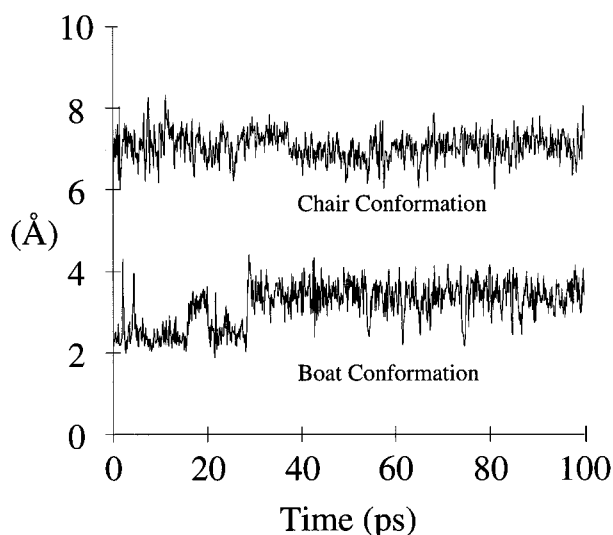


**Figure 5.** Proton-anomeric oxygen distance for the two stable hexaNAG conformations during the dynamics simulation. Proton transfer is likely for the  $-1$ -boat geometry only. Note the small fluctuations in these distances which indicates a stable trajectory during the simulation.

Evidence in support of this includes the observation that Glu 315 is completely conserved in family 18 chitinases. In addition, site-directed mutagenesis of the corresponding Glu residue in the *Bacillus circulans* chitinase to a Gln was reported to essentially eliminate activity.<sup>37</sup>

For the chitinase system, the likelihood of proton transfer primarily depends on the distance between the proton donor and acceptor. Making the assumption that Glu 315 is the donor, the proposed proton acceptor is the  $\beta$ -(1,4)-glycosidic oxygen between sugar residues  $-1$  and  $+1$ . A plot of the proton-

oxygen distance for the hexaNAG simulations is shown in Figure 5. It is evident that the extended *N*-acetyl geometry of the  $-1$ -chair conformation places the glycosidic oxygen too far from Glu 315 (7 Å) for efficient proton transfer. In contrast, the  $-1$ -boat geometry places the proton between 3 and 4 Å away from the glycosidic oxygen and occasionally much closer when a direct hydrogen bond is made. From these simulations, it may be concluded that binding of a chitin substrate in the  $-1$ -chair geometry is not compatible with protonation. Such a binding event would not lead to rapid hydrolysis.

**4.2 Substrate Distortion.** A basic tenet of enzyme catalysis states that the catalytic rate enhancement achieved by an enzyme is a result of preferential binding (stabilization) of the transition state relative to the substrate.<sup>38</sup> In some instances, initial binding may induce a geometrical distortion in the glycosyl substrate. Evidence has been reported supporting the role of substrate distortion for influenza virus neuraminidase,<sup>39,40</sup> endoglucanase I,<sup>27</sup> bacterial chitinase,<sup>26</sup> and 1,3- $\beta$ -glucanases<sup>41</sup> and suggested for hen lysozyme.<sup>14</sup> We find that tight binding of the  $-1$ -boat hexaNAG substrate distorts the sugar residue at subsite  $-1$  to induce a boat conformation (Figure 4). This is not observed for any other GlcNAc residues, all of which prefer the lower energy chair conformation.

The boat conformation observed for hexaNAG residue  $-1$  is a consequence of several factors. A complementary fit of the  $-1$ -boat *N*-acetyl geometry to the active site pocket is essential and anchors C2' in place. C4' and C1' are prevented from assuming the more favorable chair conformation due to the steric clash between the binding site cleft and hexaNAG residues  $+1$  and  $+2$ . Indeed, upon removal of residues  $+1$  and

(38) Wolfenden, R. *Nature* **1969**, 223, 704.

(39) Varghese, J. N.; McKimmin-Breshkin, J. L.; Caldwell, J. B.; Kortt, A. A.; Colman, P. M. *Proteins* **1992**, 14, 327-332.

(40) Burmeister, W. P.; Ruigrok, R. W. H.; Cusack, S. *EMBO J.* **1992**, 11, 49-56.

(41) Hrmova, M.; Garrett, T. P. J.; Fincher, G. B. *J. Biol. Chem.* **1995**, 270, 14556-14563.

(37) Watanabe, T.; Kobori, K.; Miyashita, K.; Fujii, T.; Sakai, H.; Uchida, M.; Tanaka, H. *J. Biol. Chem.* **1993**, 268, 18567-18572.

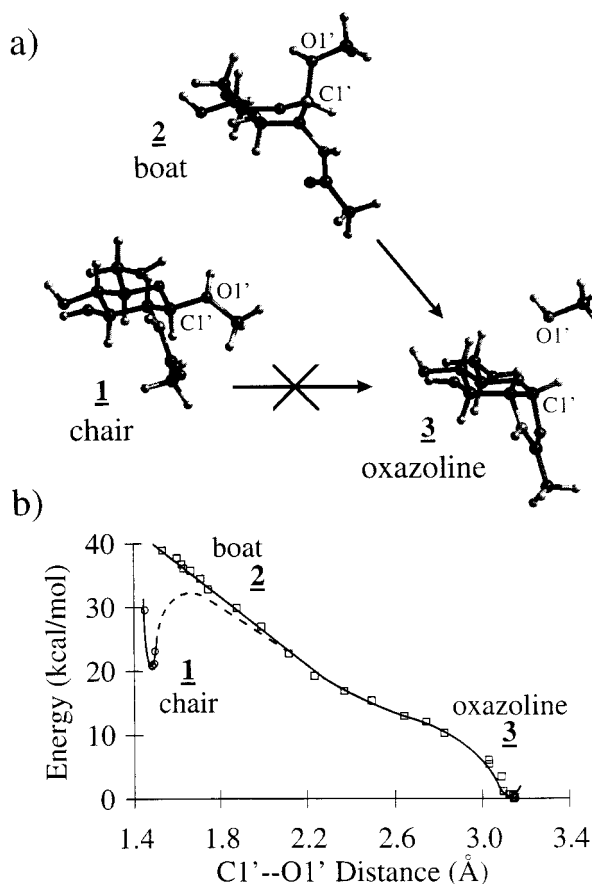


**Figure 6.** (a) (1) The optimized methyl-substituted GlcNAc oxonium ion in a chair conformation. (2) The protonated boat conformation prior to glycosidic bond cleavage and formation of an oxazoline ion. (3) The optimum oxazoline ion-methanol complex. Absolute energy of **3** is  $-854.726\ 515$  hartree. The optimized chair conformation (**1**) is 20.8 kcal/mol higher in energy than the oxazoline ion. (b) A plot of relative energy versus the C1'-O1' distance during geometry optimization. The local minimum about the chair conformation is visible, and no barrier between the protonated boat and the oxazoline ion is observed.

+2, molecular mechanics minimization of the remaining tetraNAG substrate reveals that the sugar at subsite -1 now prefers a chair conformation.

There is considerable debate regarding the significance of such substrate distortion for enzyme catalysis by the glycosyl hydrolases.<sup>42</sup> A recently reported QM study of 2-oxanol<sup>43</sup> suggests that substrate distortion determines the mechanistic path of acid-catalyzed glycosidic cleavage. Protonation of a chair conformation follows a stepwise path to a stable (high-energy) oxonium ion which then dissociates to an oxocarbenium ion. Protonation of all other sugar conformations induces a concerted dissociation leading directly to an oxocarbenium ion.

We have extended this work to include O1'-methyl-GlcNAc. Geometry optimization starting from a boat conformation, **2** (Figure 6a), leads directly to bond cleavage and the formation of an oxazoline ion/methanol complex, **3** (Figure 6a). The analogous optimization starting from a chair geometry does not lead to bond cleavage, but rather a stable oxonium ion (**1**), as was observed for 2-oxanol. Figure 6b shows a plot of the relative energy versus the C1'-O1' distance (monitored during the geometry optimization). The chair conformation remains

in a local minimum 20.8 kcal/mol above the oxazoline ion-methanol complex.

In light of this QM data and our simulation results, it is reasonable to suggest that substrate distortion is a critical component of the oxazoline double displacement mechanism. However, in the presence of a 2'-N-acetyl with a favorable orientation, we propose protonation of a boat conformation will result in a concerted dissociation directly to an oxazoline ion with little or no barrier. For the purpose of the molecular dynamics simulations, we have assumed a stepwise mechanism in which proton transfer is followed by bond cleavage and formation of the oxazoline ion intermediate. Although these studies show that such a stepwise mechanism is allowed, they do not rule out the possibility of a completely concerted reaction mechanism with the proton transfer and glycosidic bond cleavage occurring simultaneously.

**4.3 Active Site Structure.** A model of the chitinase active site was proposed based on the X-ray structure of Chitinase A complexed with tetraNAG (*N,N,N',N''*-tetraacetylo-chitotetraose).<sup>2</sup> The crystal structure revealed only one sugar residue bound, perhaps because of hydrolysis of the substrate or disorder. Using this limited data, a model was generated on the basis of the assumption that this sugar was bound to subsite -1. An alternative model was suggested in which this sugar was a product of the reaction and hence bound to subsite +1. However, this was subsequently dismissed on the basis of poor electron density for a second bound sugar which would indicate the occupation of two "product" sites leaving the four remaining "substrate" sites unoccupied.

Our simulation results are consistent with a model in which the sugar observed by X-ray crystallography does indeed occupy subsite +1, not subsite -1. This is not a surprising result after considering the recent analysis of the conserved sequence and structure motifs for six family 18 glycosyl hydrolases.<sup>13</sup> This analysis allows an alignment to be made between Chitinase A and hevamine. Detailed structural information is available for hevamine including X-ray structures of a hevamine-triNAG complex and hevamine-allosamidin complex. Five of the six residues forming the active site of hevamine are conserved, therefore extrapolation to Chitinase A is trivial.

The reported electron density of the sugar residue observed by crystallography supports our model for sugars +1 and +2 of the -1-boat hexaNAG system. The most striking conformational feature of these two sugar residues is the twist induced between residues -1 and +1. The binding of residues +1 and +2 is reminiscent of that observed for HEWL, in which the sugars are parallel with the binding cleft. In contrast, the plane defined by the pyranose rings of sugar residues -4 through -1 is perpendicular to the binding cleft. This helps to induce the boat conformation observed for sugar -1 and may further strain the glycosidic linkage at that point.

**4.4 Potential Products from Reaction Intermediates.** Although we have presented considerable theoretical evidence in support of an oxazoline ion intermediate, it is still useful to compare the predicted products of each possible intermediate. In our simulations, the oxazoline ion and -1-boat derived oxocarbenium ion both present the same solvent accessible surface. As a result of steric constraints of the active site pocket, nucleophilic attack by water would be predicted to yield exclusively the  $\beta$ -anomer (Figure 7a). This agrees with the experimentally observed product.

We predict that the -1-chair-derived oxocarbenium ion intermediate with an "extended" *N*-acetyl geometry will not occur. However, if such a species were to arise, our simulations

(42) For a discussion of the importance of substrate distortion, see: Frestle, A. *Enzyme Structure and Mechanism*; W. H. Freeman and Co.: New York, 1985; pp 336-338, 435-436, and references therein.

(43) Smith, B. *J. Am. Chem. Soc.* **1997**, *119*, 2699-2706.

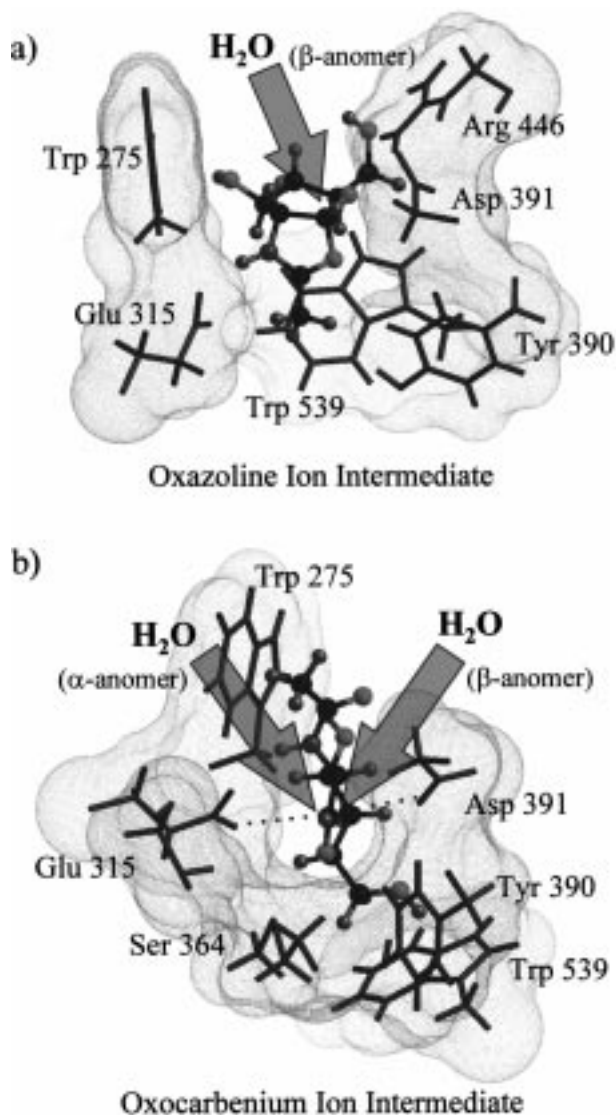


**Figure 7.** (a) The oxazoline ion intermediate bound to the chitinase A active site, shown with a vdW surface. Only one face of the oxazoline ion is open to attack by water at C1' (as indicated with an arrow) which will lead to a single anomeric product. (b) The extended oxocarbenium ion intermediate is stabilized by Glu 315 and Asp 391 (dotted line), and the active site cleft is more narrow than for the oxazoline ion. Attack by water at C1' is hindered equally on both sides of the cleft (as indicated by two arrows) and will likely yield a mix of anomeric products.

indicate the hydrolysis product would be a mix of  $\alpha$ - and  $\beta$ -anomers. Both faces of the oxocarbenium ion are equally solvent accessible (Figure 7b). In addition, there are no specific side chain interactions which could exert a significant preference for nucleophilic attack by water from one side over the other as Glu 315 and Asp 391 are a similar distance from C1' (3.19 and 3.04 Å, respectively). A slight preference for the  $\beta$ -anomer may be induced by Trp 275 which flanks a portion of the binding site. Therefore, the products predicted for an oxocarbenium ion intermediate are inconsistent with the reported experimental results.

**4.5 Design of a New Class of Inhibitor.** The inhibition of chitinases has been identified as a possible objective in the development of novel antifungal therapeutics.<sup>10</sup> When considering the rational design of a family 18 chitinase inhibitor, it is useful to identify unique points along the hydrolysis pathway which may be targeted. Two such points are the distorted boat

conformation assumed at subsite -1 and the oxazoline ion intermediate. Indeed, inhibitors which mimic an oxazoline ion intermediate have been identified in the allosamidin family of natural products.<sup>10,23,44</sup> The allosamidins have been reported to be potent chitinase inhibitors, and we have shown, using ab initio QM, that allosamidin shares characteristic structural and electronic properties of the oxazoline ion.<sup>24</sup>

On the basis of our Chitinase A simulations, we suggest an alternative inhibitor may be designed to mimic the substrate bound at subsite -1 prior to protonation. The key structural features to be included in such a design are the following:

- (1) a constrained pyranose ring in a boat conformation (possibly through a substituted bicyclo[2.2.2]octane),
- (2) an *N*-acetyl group in a position equivalent to C2' of GlcNAc, and
- (3) a hydrogen bond acceptor for proton on Glu 315.

Further modifications could be made in an attempt to occupy the "substrate" and "product" binding sites -3 through +2. In the case of the allosamidins, only the "substrate" sites are occupied. This inhibitor has the additional benefit of being neutral whereas the oxazoline ion is positively charged.

## 5.0 Conclusion

We have applied MD simulation methods to Chitinase A complexed with different hexaNAG substrate conformations and reaction intermediates. The results of these simulations offer considerable insight to the understanding of the hydrolysis mechanism. Protonation of the hexaNAG substrate by Glu 315 is likely to occur only for the -1-boat binding mode. The -1 sugar residue is distorted to a boat conformation by tight binding of the *N*-acetyl group and steric constraints between sugar residues +1 and +2 and the enzyme binding cleft. In addition, the planes of sugar residues -1 and +1 are twisted 90° relative to one another, placing strain on the glycosidic linkage. QM data (HF/6-31G\*\*) indicates that protonation of the distorted hexaNAG substrate leads to cleavage of the glycosidic bond and formation of an oxazoline ion in a concerted reaction mechanism with little or no barrier.

We previously suggested the possibility of an oxazoline ion intermediate based on the crystal structure of an allosamidin-hevamine complex and QM data. The allosamidins are potent inhibitors of some chitinases and are presumably transition state analogues of the oxazoline intermediate. We now suggest an alternative inhibitor design targeted against the initial hexaNAG binding event. Such an inhibitor would have preorganized structural features which take advantage of the need for a distorted boat conformation and have a neutral charge.

**Acknowledgment.** We are grateful to Professor Barbara Imperiali for many helpful discussions. This research was initiated with funding by DOE-BCTR (DE-FG36-93CH105 81, David Boron) and completed under NSF-CHE 95-22179. The facilities of the MSC are also supported by grants from NSF (CHE 95-22179 and ASC 92-100368), Chevron Petroleum Technology Co., Saudi Aramco, Asahi Chemical, Owens-Corning, Exxon, Chevron Chemical Company, Chevron Research and Technology Co., Avery-Dennison, Hercules, BP Chemical, and Beckman Institute.

**Supporting Information Available:** Atomic coordinate files (PolyGraf and PDB format) for the optimized hexaNAG/chitinase structures and triNAG-intermediate/chitinase structures

(44) Sakuda, S.; Isogai, A.; Matsumoto, S.; Suzuki, A. *Tetrahedron Lett.* **1986**, 27, 2475-2478.

(45) Tews, I.; Terwisscha van Scheltinga, A. C.; Perrakis, A.; Wilson, K. S.; Dijkstra, B. W. *J. Am. Chem. Soc.* **1997**, 119, 7954-7959.

are available through the Web only and may be downloaded from the publications section of the <http://www.wag.caltech.edu/> website. See any current masthead page for ordering information and Web access instructions.

**Note Added in Proof.** While this paper was under review, Tews et al.<sup>45</sup> published a study comparing the X-ray crystal

structures of glycosyl hydrolase families 18<sup>2,22,23</sup> and 20<sup>26</sup> with bound substrates. Their findings are in complete agreement with the theoretical models proposed in this work and further validate a role for substrate distortion in the mechanism of family 18 chitinases.

JA972282H